RSC Advances

ROYAL SOCIETY OF CHEMISTRY

www.rsc.org/advances

Journal Name

ARTICLE TYPE

Cite this: DOI: 10.1039/xxxxxxxxxx

Received Date
Accepted Date

DOI: 10.1039/xxxxxxxxxx

www.rsc.org/journalname

Indiene 2D Monolayer: a New Nanoelectronic Material

Deobrat Singh,[a] Sanjeev K. Gupta,[b] Igor Lukačević,*[c] and Yogesh Sonvane[a]

One atom thick monolayer nanostructures consisting of group III, IV and V elements are drawing ever more attention for their extraordinary electronic properties. Through first principles calculations, we systematically investigate structural and electronic properties of the corresponding indium monolayers in three different allotropic forms: planar, puckered and buckled. Our study shows that planar and buckled allotropes are stable and show metallic and semiconducting behavior, respectively. Their stability and electronic properties cannot be easily correlated to those of similar elemental monolayer structures. Van Hove singularity is observed in the electronic density of states which could lead to an increase in the electronic conductivity, opening paths to new electronic applications. Strain engineering is applied in order to determine the changes in the electronic behavior and band gap properties. Planar allotrope remains metallic under both compressive and tensile strain, while buckled allotrope changes from an indirect semiconductor to a metal. Our study demonstrates that the indiene nanostructures possess diverse electronic properties, tunable by strain engineering, which have potential applications in nanoelectronics and for nanodevices.

1 Introduction

Since the discovery of graphene[1–3] other two-dimensional (2D) group-III, IV and V nanostructures have attracted a lot of interest from physicists, chemists, and material scientists[4–6]. One of the trends in today's materials science is predicting two-dimensional materials, consisting of only one or two elements, which are possible candidates for a wide range of applications: from electronic devices, like field effect transistors (FET) or bipolar junction transistors (BJT), through optoelectronic devices, like light emitting diodes (LED) or solar cells, to nanomaterials science. The most important feature of these novel materials is that they possess an intrinsic band gap, contrary to graphene which suffers from its absence and, thus, has limited practical applications. This band gap is usually indirect, but it has been shown that it can be easily modified and converted to a direct band gap or even closed using strain or external electric field. Further tuning can be obtained by changing the number of layers or the stacking order of layers.

Recently, arsenene and antimonene, which are single-atom-thick layers of arsenic and antimony, have been proposed as new members of group-V monolayer nanostructures[7–11]. These arsenic[8,12] and antimony[13] nanosheets have a buckled or a puckered structure, similar to those of blue or black phosphorene, respectively[14–16]. Their buckled and puckered allotropes behave as indirect semiconductors with band gaps in the range between 0.3 and 1.6 eV. An indirect to direct band gap transition or its closing has been proposed under the influence of strain, contrary to the case of phosphorene, where a direct to indirect band gap transition has been proposed[14]. Previously considered group-IV single-element monolayer structures (apart from carbon's graphene) refer to Si (silicene), Ge (germanene) or Sn (tinene) atoms[17,18]. They exhibit buckled monolayer structures due to the hybridization of sp^2 and sp^3 orbitals. Much progress has been done in the case of these materials as they have already been experimentally verified, although only on substrates and not as the standalone materials[19–21]. They have much larger band gap than graphene, due to their low-buckled geometry and larger atomic intrinsic spin-orbit coupling strength, in the range up to 0.1 eV, which is on the other hand much smaller than in the case of group-V monolayer materials. However, they draw attention as Dirac materials with quantum spin Hall effect and a band gap which is easily tunable using external electric field[22] or by doping[23]. Up to now, out of group-III elements only aluminium has been used to predict a monolayered material - aluminene[24]. Aluminene has only one stable allotrope with a planar structure. It behaves as a metal with specific features in the electronic density of states which could point to the occurrence of chiral superconductivity. Monolayer materials consisting of other group-III elements are only mentioned in literature not to be stable in any so far considered allotropic structure, but the arguments are not published.

In this paper we study the monolayered materials made of indium atoms, named indiene in analogy with previously reported

[a] Department of Applied Physics, S.V. National Institute of Technology, Surat, India.
[b] Department of Physics, St. Xavier's College, Ahmedabad, India.
[c] Department of Physics, University J. J. Strossmayer, Osijek, Croatia. Fax: 385 31232701; Tel: 385 31232713; E-mail: ilukacevic@fizika.unios.hr

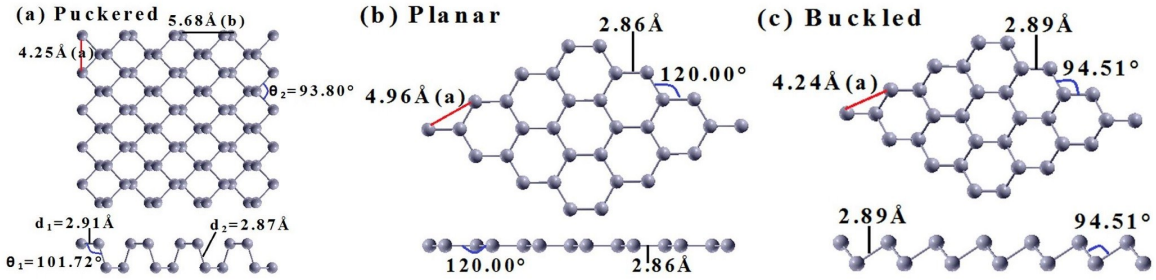

Fig. 1 Optimized geometries of (a) puckered, (b) planar and (c) buckled indiene. The red lines indicate the equilibrium lattice constants.

similar materials. Indium is considered because: (1) it is a soft, silvery metal that is stable in air and water; (2) it is widely applied as a low melting point metal alloy in industrial applications; (3) it is used in the production of transparent conductive coatings of indium tin oxide (ITO) on glass, an important part of photoelectronic industry; (4) indium nitride, phosphide and antimonide are semiconductors used in transistors and microchips, the basics of electronic applications; (5) it is used as a coating for bearings in high-performance aircraft engines, fusible alloys and in solders. All these applications bring forth indium as a suitable candidate for a graphene-like monolayer material. But what kind of structures are energetically and dynamically stable in indiene? Does the indiene nanosheet have different electronic band structure features from the other known 2D nanosheets? Can it have high carrier mobility akin to graphene? To address these questions, we perform on a first-principle theoretical investigation of the structural and electronic properties of indiene nanosheets in three different structures: planar, puckered and buckled.

Experimentally very large strains (up to 30%) can be applied to 2D layers[25–27]. These experimental studies confirm that strain engineering can be a very practical and useful path to modulate the electronic properties of 2D materials. Thus, we further focus on the effect of strain on the electronic band structures of stable indiene allotropes and its influence on the band gaps along with specific features exhibited by the electronic densities of states.

2 Computational details

We use the first principle calculation based on fully self-consistent density functional theory (DFT)[28,29] were carried out by using QUANTUM ESPRESSO package[30]. The generalized gradient approximation (GGA) in the form of Perdew-Burke-Ernzerhof (PBE)[31] exchange-correlation potential has been applied. We use the norm conserving pseudopotential for an In atom with scalar-relativistic effect as available on QUANTUM ESPRESSO web page. All three structures of indiene are periodic in xy-plane and a vacuum space of 18 Å was applied in the z-direction to restrict the interaction between two adjacent planes introduced by Born-von Karman periodic conditions in the supercell approach employed during the construction of monolayers. Electron wavefunctions were expanded in the plane wave bases sets. The kinetic energy cutoff used for the plane wave basic sets is: 30 Ry, 45 Ry and 45 Ry, for planar, buckled and puckered structure, respectively. These basis sets gave us the total energies converged up to: $3.5 \cdot 10^{-7}$ Ry, $1.5 \cdot 10^{-4}$ Ry and $4.6 \cdot 10^{-5}$ Ry, for planar, buckled and puckered allotrope, respectively. We approximate the Brillouin zone integration in reciprocal space using discrete Monkhorst-Pack meshes with $31 \times 31 \times 1$ k-points for planar and buckled, and $37 \times 37 \times 1$ k-points for puckered system. We use 10^{-10} Ry in self-consistent field calculation for convergence of the total energy. The forces on each atom are converged below 0.01 eV/Å during the structural optimization of both unit cell dimensions and atomic internal coordinates. All geometric structures were plotted using XCRYSDEN software[32]. Lattice dynamics calculations (the phonon spectrum, the density of states) are performed within the framework of the self-consistent density functional perturbation theory (DFPT)[?]. We use the same cutoff energies as in total energy calculations, which are sufficient to keep the errors in vibrational frequencies bellow 5 cm^{-1}. In order to understand the detailed features of the phonon spectra, force constant are obtained on a $5 \times 5 \times 1$ q-point mesh. The dynamical matrices at arbitrary wave vectors are obtained using Fourier transform based interpolations.

3 Results and discussion

3.1 Structural properties and stability of indiene

First we present the results of the structural optimization of all three indiene structures: planar, buckled and puckered, and their relative stability concerning their total energies and lattice dynamics. The planar allotrope is like graphene's honeycomb structure, while buckled and puckered allotropes are constructed in analogy with similar structures formed by elements like arsenic, phosphorous, silicon or germanium. The flat structure of graphene in 2-dimensional honeycomb structure has pure sp^2 hybridization. All studied structures have each indium atom bonded with other three indium atoms. The optimized geometric structures are shown in Figure 1. After optimization, the relaxed lattice constants are a = 4.25 Å, b = 5.68 Å for puckered structure, 4.96 Å for planar structure and 4.24 Å for buckled structure (Table 1). Comparison with similar monolayer structures of neighbouring elements shows that they follow the same trends as their bulk counterparts. Tin has the largest bulk lattice constant of 5.82 Å, and its buckled form, tinene[18], has larger unit cell then buckled indiene. Similarly, bulk indium has larger lattice constant (4.59 Å) than bulk aluminum (4.05 Å), and so does its monolayer form, planar indiene, regarding the planar aluminene[24]. The calculated puckered angle for puckered allotrope of indiene is 101.71°, which lies between arsenene's 100.80° and phospho-

Table 1 Structural parameters of indiene allotropes compared to similar materials: aluminene[24], tinene[18], arsenene[8], antimonene[13] and phosphorene[14]

Allotr.	Elem.	E_{coh} (eV/atom)	Latt. const. (Å)		Bond leng. (Å)	Bond ang. (deg)
			a	b		
Planar	In	−1.81	4.96	-	2.86	120
	Al	−1.96	4.49	-	2.59	120
	As	−2.39	4.37	-	2.52	120
Buckled	In	−1.83	4.24	-	2.89	94.51
	Sn	-	4.52	-	2.70	113.50
	As	−2.99	3.61	-	2.50	92.22
	Sb	−4.57	4.01	-	2.84	89.90
Puckered	In	−1.88	4.25	5.68	2.91,2.87	101.71,93.80
	As	−2.95	3.68	4.77	2.50,2.49	100.80,94.64
	Sb	−4.63	4.48	4.31	2.91,2.83	102.50,95.00
	P	-	4.63	3.29	2.25,2.22	104.25,95.89

rene's 104.25°. Another angle in puckered structure is 93.80°, which is slightly lesser in value than arsenene's 94.64°. In our case the calculated buckling height and angle are 1.54 Å and 94.51°, respectively. This angle is slightly larger than that of arsenene's 92.22°. Structural parameters of indiene and other similar materials for comparison are presented in Table 1.

Next we study the stability of all three structures of indiene. The calculated ground state total energies are -53.73, -53.66 and -53.69 eV/atom for puckered, planar and buckled allotrope, respectively. In all these cases the ground states energies of indiene are nearly equal (Figure 2). This means that, from the total energy point of view, all three structures could be stable.

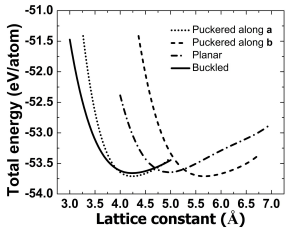

Fig. 2 Total energy of indiene allotropes as a function of lattice constants

To confirm the stability of studied structures we further regard the lattice dynamical stability of indiene monolayer allotropes by calculating their full phonon dispersion curves. As seen in Figure 3 planar and buckled structures of indiene have all real phonon frequencies. Puckered structure, on the other hand, shows imaginary frequencies for acoustic and some optic phonon modes throughout the whole Brillouin zone, similar to aluminene case[24]. Thus, the puckered structure is not lattice dynamically stable allotrope of indiene and for that reason our simulations indicate that it is not possible to obtain it using one of the above mentioned experimental techniques. Generally speaking, the stability of different allotropes of 2D graphite-like monolayer structures is very sensitive with respect to the electronic structure of element in hand. For example, tinene is unstable in its planar allotrope. Cai et al[18] stressed out the importance of buckling in stabilizing the planar allotrope. However, this is not so in indiene, consisting of indium atoms which have only one electron less than tin in the fifth electronic shell. Even more remarkably, it is completely opposite in aluminene[24], having a isoelectronic structure with indium, with a stable planar and unstable buckled allotropes. Lattice dynamical stability of other elements varies diversely, suggesting also the role of electron-phonon coupling, similarly to the one played in graphene[33,34]. Phonon dispersion curves of buckled indiene resemble those of buckled tinene and antimonene, with separated acoustic and optic branches. Optic phonon modes are, however, less dispersed. Planar indiene allotrope contrasts that of aluminene in the optic mode which is separated from other optic modes, while in aluminene it approaches them at the K point of the Brillouin zone. Since the indiene in puckered configuration is not stable, as observed from its phonon spectra, we do not consider it for further analysis.

Graphene is manufactured by exfoliating graphite. Recently, phosphorene has also been manufactured by exfoliating black phosphorus[35–37], similarly to the case of graphene[38]. Bulk indium has a body centered tetragonal unit cell (I4/mmm). It can be viewed as two planes of same atoms, shifted by 1/4 of the unit cell length (in each direction, respectively) respect to each other. If separated from the bulk, each pair of these two planes has exactly the same structure as the buckled monolayer of indium atoms. Thus, it may be possible to obtain the buckled indiene by exfoliating indium. Since the ground state total energies of both planar and buckled indiene are very close to the bulk indium, the possibility of manufactured those indiene allotropes experimentally also exists. Our theoretical research brings motivation for experimental researchers to grow indiene.

3.1.1 Buckled indiene.

3.2 Band structure

The electronic band structures, density of states (DOS) and partial density of states (PDOS) for two stable structures: planar and buckled, with the equilibrium lattice constants have been calculated. Electronic band structures together with the DOS and PDOS of individual orbitals of electronic states are shown in Figure 4. Planar form behaves like a metal due to partial occupancies of hybrid sp^2 orbitals (σ and π). Two Dirac cones appear at the K point, at around 1.5 and -4.9 eV. The former one belongs to π bonds consisting primarily of p_z orbitals, while the later one belongs to σ bonds having contributions from s and somewhat

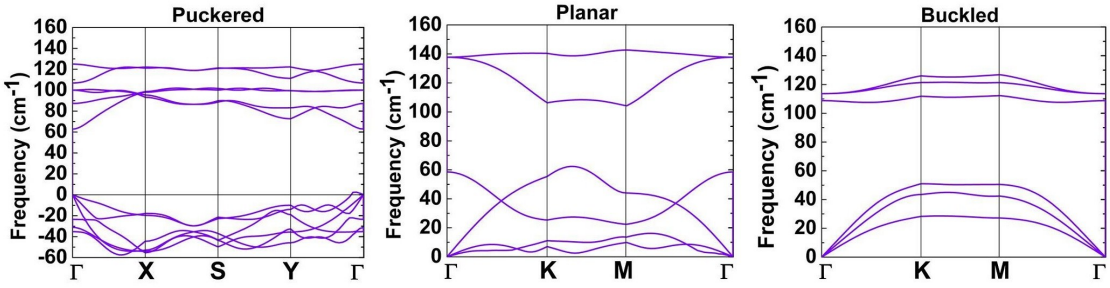

Fig. 3 Full phonon dispersion curves of puckered, planar and buckled allotropes of indiene.

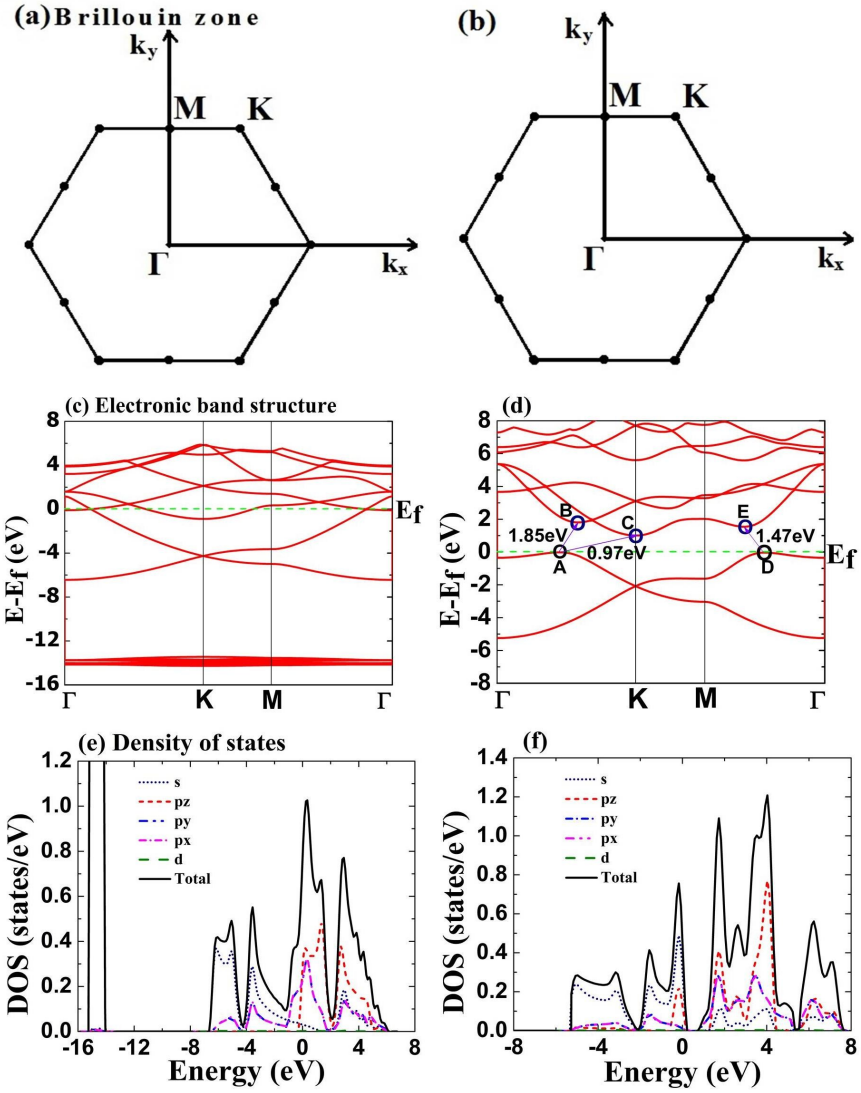

Fig. 4 Electronic properties of stable indiene allotropes. The hexagonal Brillouin zones of (a) planar and (b) buckled allotrope with high symmetry k-points. The electronic band structures of (c) planar and (d) buckled indiene with the Fermi level set to zero. Total DOS and partial DOS of (e) planar and (f) buckled indiene.

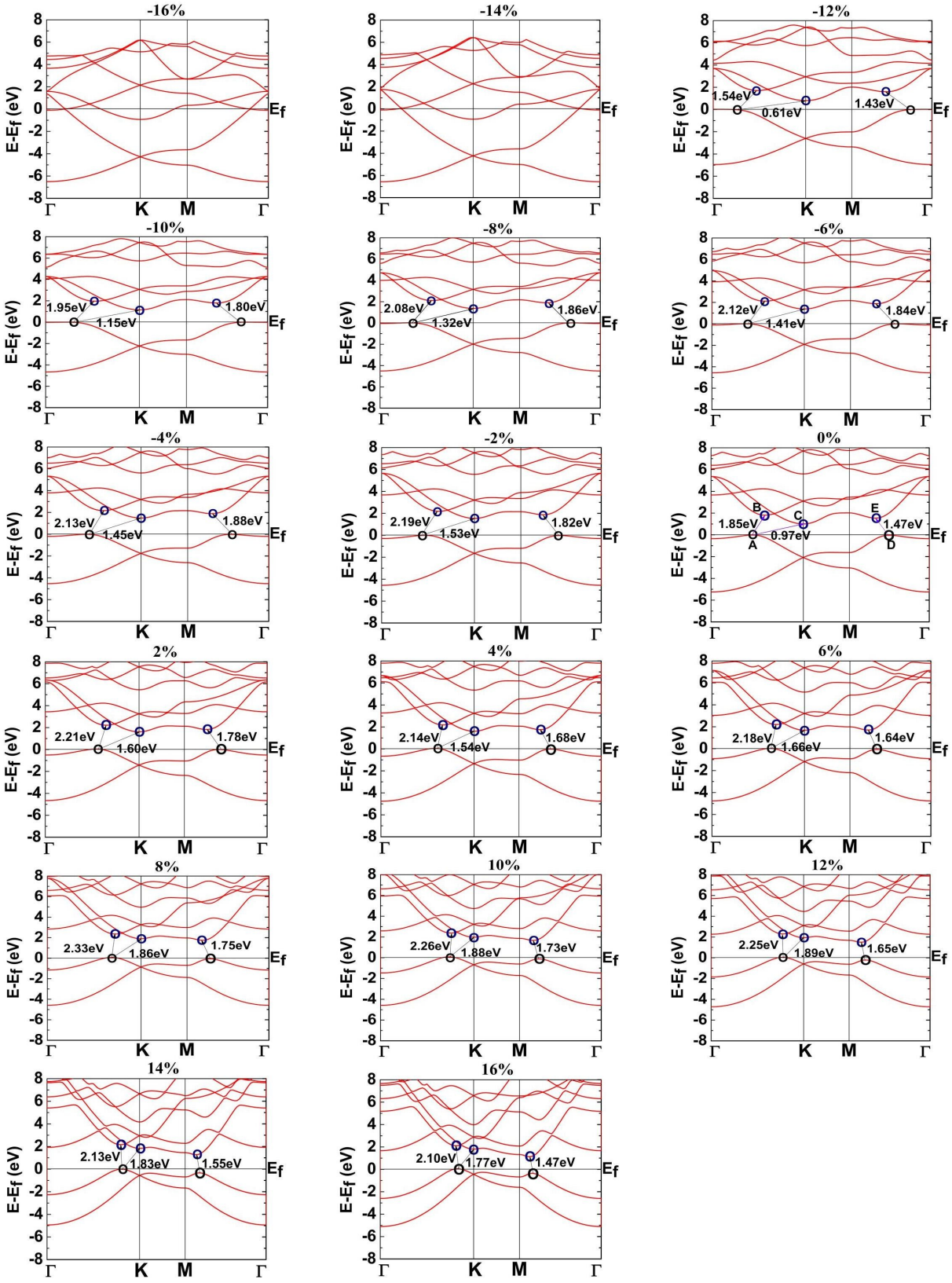

Fig. 5 The variation of electronic band structure with strain in buckled indiene.

less from p_x and p_y orbitals. Two σ bands cross the Fermi level. Higher energy one belongs to p orbitals, while the lower energy one belongs to s, p and d orbitals. Dominance of p orbitals around the Fermi level is a common characteristic of 2D monolayer compounds, formed by sp^2 hybrid bonds, like silicene and phosphorene [19,39]. From the application point of view, a remarkable feature can be observed in electronic DOS (Figure 4(e)). A van Hove singularity of the p orbital is found at the energy of about -0.2 eV, very close to the Fermi level. If one could shift the Fermi level so that it coincides with the van Hove singularity, one would obtain a very large electrical conductivity with an application of gate voltage [40].

On the other hand, buckled form behaves like an indirect semiconductor, as small gaps appear as seen in Figure 4(d). If one looks in the direction from Γ to K point, there are two energy gaps illustrated using points A (valence band maximum), B and C (conduction band minimum). A gap between the points A and B is 1.85 eV and between A and C it is 0.97 eV. In the direction from M to Γ point there is one energy gap between the points D and E, which is 1.47 eV. The energies of these bands, i.e. the positions of the above defined points are critical for the semiconducting character of buckled indiene. Valence band maximum (VBM) shows a character of almost pure s states close to -3 eV (Fig 4(f)). Conduction band minimum (CBM) has a hybrid character of dominant p states and non-negligible contribution of s and d states.

In the next subsection we will discuss the effect of strain on the electronic band structures of planar and buckled indiene. This will allow us to see the changes in the energy gaps and consequently the changes in the electronic behavior of indiene.

3.3 Band gap strain engineering

We modify the band structures and their properties by application of mechanical strain. Applying the mechanical strain on a 2D structure is an easy and convenient method for modulating it's electronic properties. Up to now, there are several theoretical studies which investigated the effect of strain on the electronic properties of monolayer structures [8,13,14,41]. Experimentally, it is known that one can induce spontaneous strain by depositing material layers on flexible substrates or by using beam-bending apparatus [42] or scanning tunnel microscope tips for tensile strain [43]. In our theoretical study strain was simulated by fixing and relaxing the respective lattice constants and atomic internal coordinates of indiene allotropes.

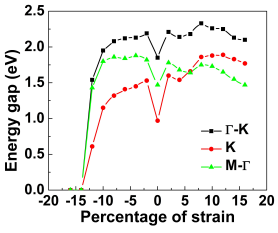

Fig. 6 Effect of strain on the band gap of buckled indiene. Electronic properties are governed by the features at K point, where the band gap closes for large tensile strains

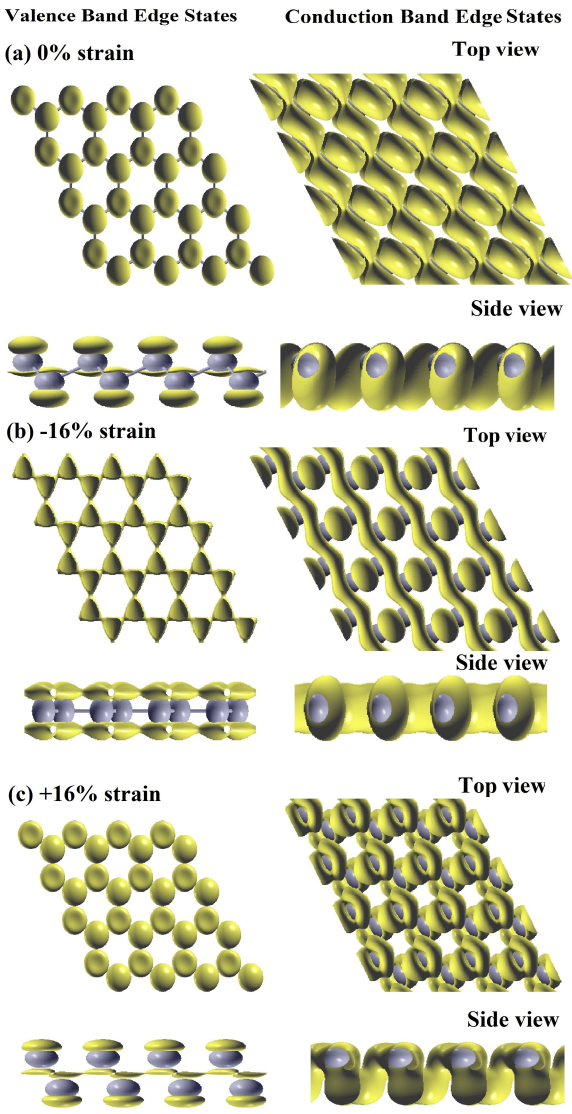

Fig. 7 The valence and conduction band charge densities of buckled indiene without strain, -16% and +16% strain in (a), (b) and (c), respectively, with top and side views of 4×4 supercell

3.3.1 Buckled indiene.

We have performed a study on the effect of strain on the electronic properties of buckled indiene. In this case we apply negative and positive strains symmetrically along its lattice vectors (biaxial strain), because buckled monolayer structures show isotropic mechanical properties [13]. Strain is taken in the steps of 2% between -16% and +16% from the unstrained geometry. This segment of strains proved to be sufficient to indicate the significant changes. All these changes can be attributed to the shifts in the near gap states. Induced strain causes the atomic distances to change. As atoms in the 2D monolayer get closer or further away from each other, so do the overlaps of electron orbitals become larger or smaller. Different overlaps cause different superpositions of these orbitals, which results in the shifts of the electron energy states. After applying the compressive and tensile strain on the optimized geometric structure, the variation of total energy of the system

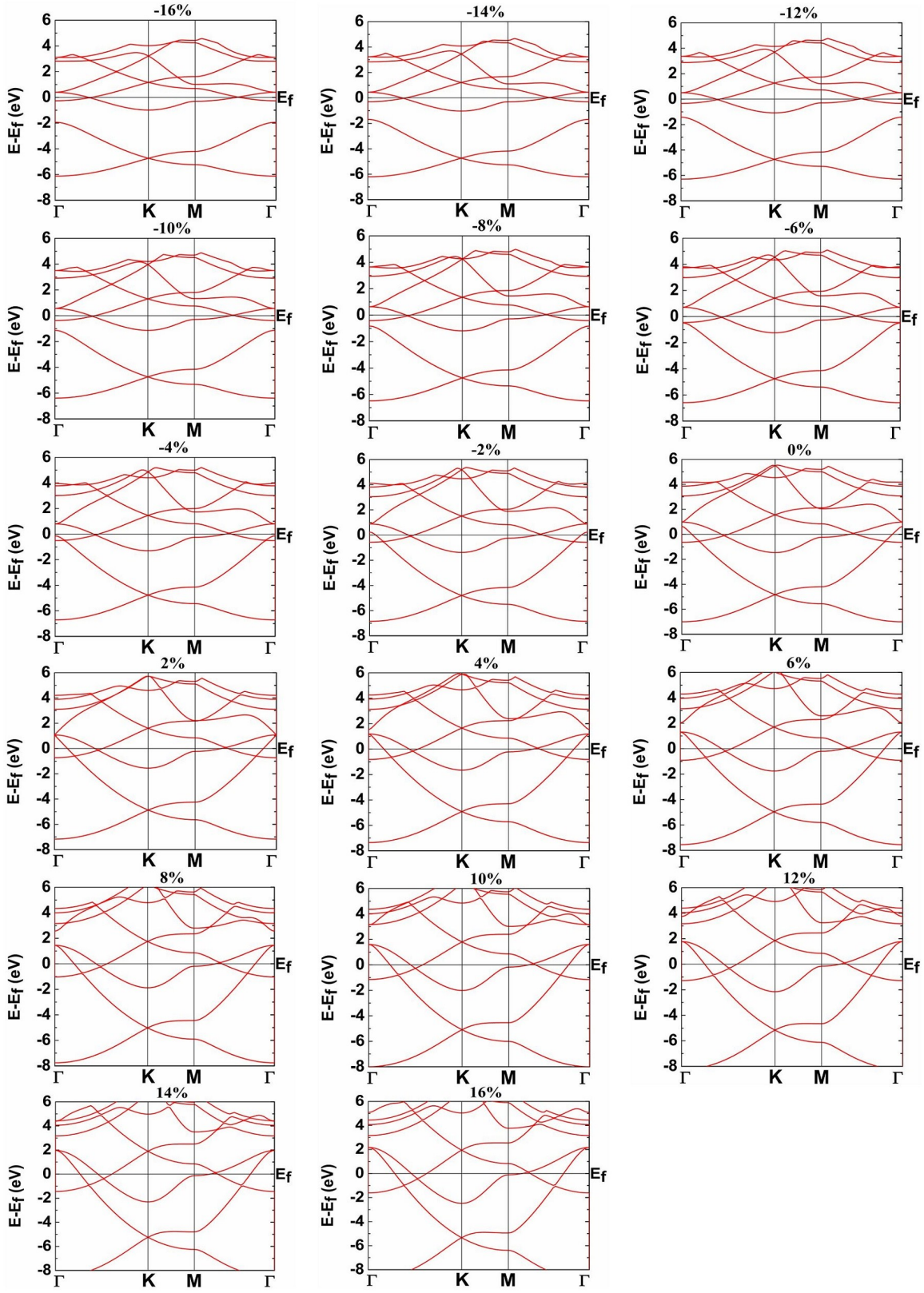

Fig. 8 The variation of electronic band structure with strain in planar indiene.

shows a parabolic form (Figure 2). This confirms the energetic stability of the strained buckled indiene allotrope. Total energy of the system is more dominant in the case of positive and less dominant in the case of negative strain.

The changes in the electronic band structure under strain are shown in Fig 5. When we apply the negative strain, the energy gap initially increases, but then starts to continuously decrease along the Γ-K and M-Γ directions as well as at the K point, and buckled indiene retains its indirect semiconductor behavior until -14% strain. Beyond this strain the band gap quickly closes at all relevant points in the band structure and buckled indiene becomes metallic. This abrupt decrease of the band gap is atributed to the phase transition during which the buckled allotrope is stretched to the planar one. These kind of transitions were already found in some monolayer materials like pentagonal B_2 [44]. In view of this, the 16% strain can be thought of as a critical strain at which the material changes its electronic behavior, i.e. it undergoes a semiconductor to semimetal transition. This transition possibly present very interesting application for engineering the electronic properties of buckled indiene. On the other side, after the initial increase, the energy gap continuously decreases between the relevant points when we apply the positive strain, but retains its semiconducting character even for large strains. The strain dependence of band gap is shown in Fig 6. In the compressive strain region it has some similarity with the band gap changes in buckled arsenene as both stop to be semiconducting. The difference is that buckled arsenene becomes a semimetal at -10% strain. In the tensile strain region the behavior is essentially different from the buckled arsenene[8] or antimonene[13], which both turn metallic, while indiene remains a semiconductor. It might be interesting to note that there are no significant shifts of VBM and CBM points inside the Brillouin zone, as found in some similar materials, like arsenene[8]. The only shift is found at point B, which shifts to the left and seems to be aligning itself with point A at strains larger than +10%, exhibiting, thus, a direct gap between VBM and CBM. However, its importance is impaired by the more significant features between points A and C as indicated above.

We would also like to compare the amount of the change in the band gap between the presently studied indiene and previously studied arsenene[8] and antimonene[13] in the form of the same buckled allotrope. Under tensile strain of +12% the band gap in indiene changes by 0.92 eV, more than half as much as in arsenene (-1.64 eV), and much closer to the change in antimonene (-0.74 eV), which has more similar electronic structure. Since buckled indiene preserves its structure under strains up to 20%, this comparison points out that an efficient band gap modulation can be achieved using in-plane strain, tuning it over a range of almost 1 eV. Using buckled indiene as an optoelectronic nanomaterial is, thus, a promising path to new devices.

Insightful way to describe the changes in the band structure is to study the electronic charge density distribution (Fig 7). Under no strain buckled indiene shows moderately localized distribution of electronic orbitals, which are somewhat distorted along the bonding directions (hexagon sides). Valence state is predominantly localized, whereas conduction state exhibits delocalized distribution of electron charge density. Charge densities change critically under mechanical strain. These changes are sufficient to induce a transition in the electronic properties. Specifically, under negative compressive strain, a large increase of delocalization of VBM state along the bonds can be observed. An increased distribution of delocalized electrons decreases the band gap until it closes for the strain of -14%. These electrons become quasi-free and are able to conduct electricity, making the buckled indiene metallic under compressive strain. Under tensile strain the changes are not so significant.

3.3.2 Planar indiene.

The effect of strain on the electronic band structure of planar indiene is shown in Figure 8. Planar indiene keeps its metallic behavior throughout the whole segment of strains used in our calculations. As expected, negative strain closes in the electronic bands, while positive strain spreads them out: valence bands toward more negative and conduction bands toward more positive energies.

Charge distribution of valence electrons is presented in Figure 9. Except the middle hexagon regions, which show no charge density accumulation, the charge is nearly uniformly extended over the two dimensional indiene plane which contributes to the conductivity. We have also calculated the difference between the charge densities of system and its atomic constituents. It clearly indicates the presence of covalent bonds, because of the high electronic densities along the bonding directions between the indium atoms.

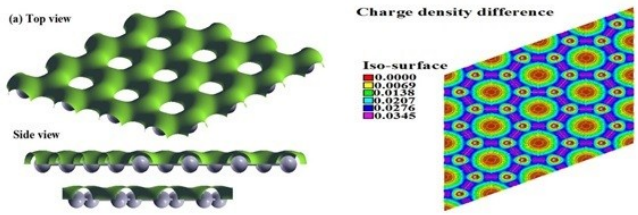

Fig. 9 Valence charge density distribution (a) of planar indiene with top and side views of 4×4 supercell. Contour lines represent the charge density differences between the total and atomic densities from 0.00 to 0.0345 eÅ^{-2}.

4 Conclusions

In conclusion, calculations based on first principles approach show that the planar and buckled structures of two-dimensional material - indiene, are stable allotropes from both total energy and lattice dynamics point of view, while the puckered one is dynamically not stable. The total energy of stable structures (planar and buckled) is nearly equal, meaning that they could both be potentially exfoliated from the bulk indium. The planar allotrope behaves like a metal, with Dirac points in the band structure and van Hove singularity in the density of states, which could practically lead to an increase in the electronic conductance. On the other hand, the buckled allotrope behaves like an indirect semi-

conductor with a band gap of almost 1 eV. Using strain engineering, this band gap can be further increased (tensile strain) or even closed (compressive strain) so that it behaves like a metal. Based on the energy band gaps in the proposed two-dimensional systems, we can predict that planar and buckled forms of indiene form good candidates for optoelectronics or nanoelectronic devices, such as memory devices, light emitting diodes and solar cells, which expect further experimental verifications.

References

1 K. S. Novoselov, A. K. Geim, S. V. Morozov, D. Jiang, Y. Zhang, S. V. Dubonos, I. V. Grigorieva and A. A. Firsov, *Nature*, 2004, **306**, 666–669.

2 A. K. Geim and K. S. Novoselov, *Nat. Mater.*, 2007, **6**, 183–191.

3 A. H. C. Neto, F. Guinea, N. M. R. Peres, K. S. Novoselov and A. K. Geim, *Rev. Mod. Phys.*, 2009, **81**, 109–162.

4 J. Qiao, X. K. X, Z. X. Hu, F. Yang and W. Ji, *Nat. Commun.*, 2014, **5**, 4475–4481.

5 G. Wang, R. Pandey and S. P. Karna, *Nanoscale*, 2015, **7**, 524–531.

6 P. Bharadwaj and L. Novotny, *Optics & Photonics News*, 2015, **July/August**, 26–31.

7 S. Zhang, Z. Yan, Y. Li, Z. Chen and H. Zeng, *Angew. Chem. Int. Ed. Engl.*, 2015, **54**, 3112–3115.

8 C. Kamal and M. Ezawa, *Phys. Rev. B*, 2015, **91**, 085423–085432.

9 Z. Zhu, J. Guan and D. Tomanek, *Phys. Rev. B*, 2015, **91**, 161404–161408.

10 Y. Wang and Y. Ding, *J. Phys.: Condens. Matter.*, 2015, **27**, 225304–225313.

11 Z. Zhang, J. Xie, D. Yang, Y. Wang, M. Si and D. Xu, *Appl. Phys. Express*, 2015, **8**, 055201–055204.

12 K. Liangzhi, Y. Ma, X. Tan, T. Frauenheim, A. Du and S. Smith, *J. Phys. Chem. C*, 2015, **119**, 6918–6922.

13 G. Wang, R. Pandey and S. P. Karna, *ACS Appl. Mater. Inter.*, 2015, **7**, 11490–11496.

14 C. Wang, Q. Xia, Y. Nie and G. Guo, *Journal of Applied Physics*, 2015, **117**, 124302–124311.

15 L. Li, Y. Yu, G. J. Ye, Q. Ge, X. Ou, H. Wu, D. Feng, X. H. Chen and Y. Zhang, *Nat. Nanotechnol.*, 2014, **9**, 372–377.

16 H. Liu, A. T. Neal, Z. Zhu, X. Xu, D. Tomanek and P. D. Ye, *ACS Nano*, 2014, **8**, 4033–4041.

17 C. C. Liu, H. Jiang and Y. Yao, *Phys. Rev. B*, 2011, **84**, 195430–.

18 B. Cai, S. Zhang, Z. Hu, Y. Hu, Y. Zou and H. Zeng, *Phys. Chem. Chem. Phys.*, 2015, **17**, 12634–12638.

19 P. Vogt, P. D. Padova, C. Quaresima, J. Avila, E. Frantzeskakis, M. C. Asensio, A. Resta, B. Ealet and G. L. Lay, *Phys. Rev. Lett.*, 2012, **108**, 155501–.

20 C.-L. Lin, R. Arafune, K. Kawahara, N. Tsukahara, E. Minamitani, Y. Kim, N. Takagi and M. Kawai, *Appl. Phys. Express*, 2012, **5**, 045802–045804.

21 A. Fleurence, R. Friedlein, T. Ozaki, H. Kawai, Y. Wang and Y. Yamada-Takamura, *Phys. Rev. Lett.*, 2012, **108**, 245501–.

22 N. D. Drummond, V. Zólyomi and V. I. Fal'ko, *Phys. Rev. B*, 2012, **85**, 075423–075429.

23 Z. Ni, H. Zhon, X. Jiang, R. Quhe, G. Luo, Y. Wang, M. Ye, J. Yang, J. Shi and J. Lu, *Nanoscale*, 2014, **6**, 7609–7618.

24 C. Kamal, A. Chakrabarti and M. Ezawa, 2015.

25 Q. Wei and X. Peng, *Appl. Phys. Lett.*, 2014, **104**, 251915–251919.

26 G. Wang, M. Si, A. Kumar and R. Pandey, *Appl. Phys. Lett.*, 2014, **104**, 213107–213110.

27 K. S. Kim, Y. Zhao, H. Jang, S. Y. Lee, J. M. Kim, K. S. Kim, J.-H. Ahn, P. Kim, J.-Y. Choi and B. H. Hong, *Nature*, 2009, **457**, 706–710.

28 P. Hohenberg and W. Kohn, *Phys. Rev.*, 1964, **136**, B864–B871.

29 W. Kohn and L. J. Sham, *Phys. Rev.*, 1965, **140**, A1133–A1138.

30 P. Giannozzi, P. Giannozziand, S. Baroni, N. Bonini, M. Calandra, R. Car, C. Cavazzoni, D. Ceresoli, G. L. Chiarotti, M. Cococcioni, I. Dabo, A. D. Corso, S. Fabris, G. Fratesi, S. de Gironcoli, R. Gebauer, U. Gerstmann, C. Gougoussis, A. Kokalj, M. Lazzeri, L. Martin-Samos, N. Marzari, F. Mauri, R. Mazzarello, S. Paolini, A. Pasquarello, L. Paulatto, C. Sbraccia, S. Scandolo, G. Sclauzero, A. P. Seitsonen, A. Smogunov, P. Umari and R. M. Wentzcovitch, *J. Phys.: Condens. Matter.*, 2009, **21**, 395502–395520.

31 J. P. Perdew, K. Burke and M. Ernzerhof, *Phys. Rev. Lett.*, 1996, **77**, 3865–3868.

32 A. Kokalj, *Comput. Mater. Sci.*, 2003, **28**, 155–168.

33 F. Mazzola, J. W. Wells, R. Yakimova, S. Ulstrup, J. A. Miwa, R. Balog, M. Bianchi, M. Leandersson, J. Adell, P. Hofmann and T. Balasubramanian, *Phys. Rev. Lett.*, 2013, **111**, 216806–216810.

34 G.-Z. Kang, D.-S. Zhang and J. Li, *Phys. Rev. B*, 2013, **88**, 045113–.

35 A. C.-G. et al, *2D Materials*, 2014, **1**, 025001–025019.

36 L. Li, Y. Yu, G. J. Ye, Q. G. X. O. H. Wu, D. Feng, X. H. Chen and Y. Zhang, *Nat. Nenotechnol.*, 2014, **9**, 372–377.

37 F. Xia, H. Wang and Y. Jia, *Nat. Commun.*, 2014, **5**, 4458–.

38 A. Hashimoto, K. Suenaga, A. Gloter, K. Urita and S. Iijima, *Nature*, 2004, **430**, 870–873.

39 Z. Zhu and D. Tománek, *Phys. Rev. Lett.*, 2014, **112**, 176802–.

40 C. Dekker, *Physics Today*, 1999, **May**, 22–28.

41 A. S. Rodin, A. Carvalho and A. C. Neto, *Phys. Rev. Lett.*, 2014, **112**, 176801–176805.

42 H. J. Conley, B. Wang, J. I. Ziegler, J. R. F. Haglund, S. T. Pantelide and K. I. Bolotin, *Nano Lett.*, 2013, **13**, 3626–3630.

43 C. Lee, X. Wei, J. W. Kysar and J. Hone, *Science*, 2008, **321**, 385–.

44 F. Li, K. Tu, H. Zhang and Z. Chen, *Phys. Chem. Chem. Phys.*, 2015, **17**, 24151–24156.

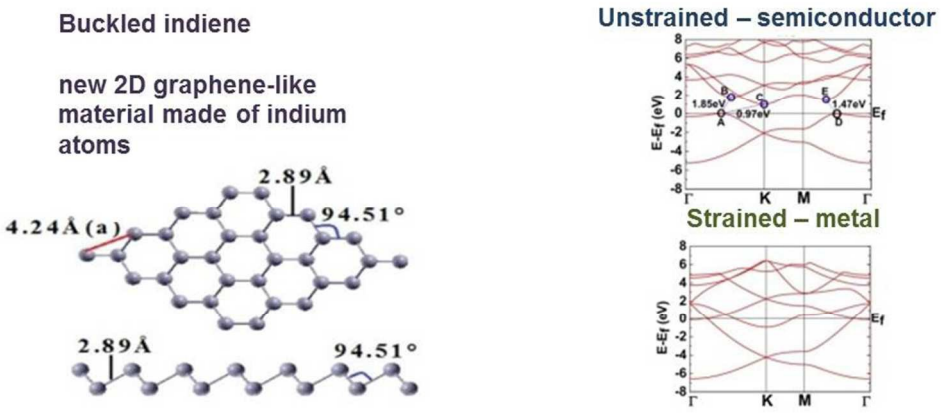

83x35mm (300 x 300 DPI)